Decaying DC and Harmonic Components Detection for Absorbing Impact Load Currents in Weak Grids

Liansong Xiong, *Member, IEEE,* Xiaokang Liu, *Member, IEEE,* and Yonghui Liu, *Student Member, IEEE*

***Abstract*—Decaying DC (DDC) current due to impact loads causes detrimental consequences in weak grids. In this paper, the active power filter (APF) is enhanced to simultaneously compensate for the undesired harmonics, negative sequence components and the DDC component in the event of a transient. To this end, first, a novel DDC component detection method is mathematically deduced for single-phase transient current, followed by its extension to the three-phase system. With respect to existing techniques, the proposed method has a significantly reduced detection time from 1 grid cycle to approximately 0.5 grid cycle. By further exploiting the transient signal properties in *dq*-frame, the three-phase fundamental-frequency current in positive sequence can be separated. Finally, the enhanced APF control scheme is developed based on the proposed DDC component detection algorithm. Experiments verified the effectiveness and advancement of the proposed technique.**

***Index Terms*—Decaying DC component, harmonic elimination, transient impact currents, power quality, active power filter.**

I. Introduction

The power quality (PQ) of utility grid is regulated by grid codes for reliable power supply. One of the PQ issues, related to the sudden topology change, is the decaying DC (DDC) component [1]. In [2], the inevitable presence of DDC component is proved by considering impact loads switching [3], especially in weak grids with high short-circuit impedance. As explanatory examples, in the event of no-load startup of a large-capacity transformer or an induction motor, or when a non-solid earth fault occurs, the instantaneous current and power can far exceed the pertinent rated level of the power grid, causing short-term overloading and heat issues of power lines and electrical equipment. Moreover, the DDC magnitude and duration depend upon the time constant of the transient circuit, as well as the grid voltage at the transient beginning [2], [4]. In the worst case, the maximum amplitude of transient current encompassing DDC components can be doubled w.r.t. the steady state [5], causing severe over-current and voltage drop issues and compromising grid safety.

To address the DDC caused impact current issues, existing solutions are categorized into passive and active ones. The former can be achieved, with the addition of passive devices encompassing reactor and resistor, by increasing the transient circuit impedance and limiting the impact current. The passive solutions are in general costly and bulky, besides they affect the steady-state current after transient. In light of development in power electronics, increasing attention is being drawn in active solutions, consisting of crowbar circuit, energy storage and active power filter (APF). Owing to the basic principle of shunting impact current in transient state and bypassing pertinent active devices in steady state, the active compensation does not influence circuit steady-state operation. Moreover, since the DDC component is eliminated by existing active devices in the grid (with a different control scheme), the additional cost is minimized. Analogous to APF annihilating harmonics, satisfactory DDC component compensation may be achieved, provided that the DDC component is accurately and timely extracted from load current signal.

Over the past few years, several methods have been developed for DDC component extraction from the transient signal, but the objective was not the detection of DDC component to be exploited for real-time compensation. Accordingly, these methods were not optimized in terms of detection time, accuracy or implementation in the embedded controller (usually a digital signal processor, i.e. DSP). The long response time of DDC component detection with empirical mode decomposition (about 2.25 grid cycles, see [5]) forbids its use in real-time compensation. The intrinsic time-scale decomposition in [4] reduces convergence time to about 1 grid cycle, yet the nonlinear minimization imposes undesirable computational burden in an APF embedded controller. The improved DFT scheme in [6] has lower computational complexity and shorter execution time, yet the estimated magnitude has a certain error and fluctuates for several grid cycles. The mathematical morphology method [7] calculates the DDC component in more than 0.5 grid cycle, yet only available at discrete points (multiples of half grid cycle). Focusing on active compensation of both harmonics and DDC currents, method in [8] requires comprehensive parameter tuning for accurate result and desired response time (about 1 grid cycle).

In this paper, a novel DDC component detection algorithm, characterized by low computational burden and feasible implementation that enables fast integration in the existing APF control system, is developed, and therefore, the APF can be enhanced for simultaneous compensation of harmonics, negative-sequence components and DDC components. With respect to existing schemes, the detection time can be reduced by nearly 0.5 grid cycle, as such effectively preventing the impact current from jeopardizing the utility grid.

II. Proposed Detection Algorithm

Without loss of generality, a single-phase transient current signal, encompassing a DDC component starting from $t = 0$ as well as odd harmonics, is considered as

$$i_{\text{tr}}(t) = I_1 \sin(\omega t + \varphi_1) + I_0 e^{-\sigma t} + \sum_{n=3,5,7,\ldots} I_n \sin(n\omega t + \varphi_n) \tag{1}$$

where I_1, ω, φ_1 are the amplitude, angular frequency and initial phase of the fundamental AC component, respectively;

I_n and φ_n the amplitude and initial phase of nth harmonic current, respectively; I_0 and σ the amplitude and decay coefficient of the DDC component, respectively.

Considering half-wave symmetry of sinusoidal signal (with T the grid cycle), the AC components can be canceled by

$$I_{\mathrm{tr}}(t) = i_{\mathrm{tr}}(t) + i_{\mathrm{tr}}(t - T/2) = I_0 e^{-\sigma t}\left(1 + e^{\frac{\sigma T}{2}}\right) \tag{2}$$

The sum current in (2) is only relevant to the DDC component. Time integrals of (2) over L and $2L$ (with $L > 0$ a specified integration period) yield

$$A_1 = \int_{t-L}^{t} I_{\mathrm{tr}}(t)\,\mathrm{d}t = \frac{I_0}{\sigma}\left(1 + e^{\frac{\sigma T}{2}}\right)\left(e^{\sigma L} - 1\right)e^{-\sigma t} \tag{3}$$

$$A_2 = \int_{t-2L}^{t} I_{\mathrm{tr}}(t)\,\mathrm{d}t = \frac{I_0}{\sigma}\left(1 + e^{\frac{\sigma T}{2}}\right)\left(e^{2\sigma L} - 1\right)e^{-\sigma t} \tag{4}$$

By combining (3) and (4), σ can be obtained as

$$\sigma = \frac{1}{L}\ln\left(A_2/A_1 - 1\right) \tag{5}$$

Substituting (5) into (2) gives the DDC current expression:

$$i_{\mathrm{DDC}}(t) = I_0 e^{-\sigma t} = \frac{I_{\mathrm{tr}}(t)}{1 + e^{\frac{\sigma T}{2}}} = \frac{i_{\mathrm{tr}}(t) + i_{\mathrm{tr}}(t - T/2)}{1 + \left(A_2/A_1 - 1\right)^{\frac{T}{2L}}} \tag{6}$$

Time integrals in (3) and (4) effectively suppress the high-frequency random noise in sampled current signal. With longer L, calculation results in (5) and (6) become more accurate, yet the detection time increases accordingly.

It should be noted that in practical applications where the grid frequency fluctuates within a narrow range (usually within 1 Hz) limited by the pertinent grid code/standard, the influence of system frequency deviation on the proposed impact current absorption scheme can be neglected.

The single-phase DDC detection algorithm can be easily extended to three-phase power systems, which is deduced as follows. For better illustration, a graphical representation of the corresponding deduction procedure is shown in Fig. 1.

Accounting also for the negative sequence components [9], the transient currents are cast as

$$\mathbf{I}(t) = \mathbf{I}_1(t) + \mathbf{I}_{\mathrm{h}}(t) + \mathbf{I}_{\mathrm{DDC}}(t) \tag{7}$$

with $\mathbf{I}(t) = \left[i_{\mathrm{tr}}^a(t) \quad i_{\mathrm{tr}}^b(t) \quad i_{\mathrm{tr}}^c(t)\right]^{\mathrm{T}}$,

$$\mathbf{I}_1(t) = I_1^+\begin{bmatrix}\sin\left(\omega t + \varphi_1^+\right)\\ \sin\left(\omega t + \varphi_1^+ - \frac{2\pi}{3}\right)\\ \sin\left(\omega t + \varphi_1^+ + \frac{2\pi}{3}\right)\end{bmatrix} + I_1^-\begin{bmatrix}\sin\left(\omega t + \varphi_1^-\right)\\ \sin\left(\omega t + \varphi_1^- + \frac{2\pi}{3}\right)\\ \sin\left(\omega t + \varphi_1^- - \frac{2\pi}{3}\right)\end{bmatrix}$$

$$\mathbf{I}_{\mathrm{h}}(t) = \sum_{n=3,5,7,\ldots}\mathbf{I}_n(t) = \sum_{n=3,5,7,\ldots} I_n^+\begin{bmatrix}\sin\left(n\omega t + \varphi_n^+\right)\\ \sin\left[n\left(\omega t - \frac{2\pi}{3}\right) + \varphi_n^+\right]\\ \sin\left[n\left(\omega t + \frac{2\pi}{3}\right) + \varphi_n^+\right]\end{bmatrix} + \sum_{n=3,5,7,\ldots} I_n^-\begin{bmatrix}\sin\left(n\omega t + \varphi_n^-\right)\\ \sin\left[n\left(\omega t + \frac{2\pi}{3}\right) + \varphi_n^-\right]\\ \sin\left[n\left(\omega t - \frac{2\pi}{3}\right) + \varphi_n^-\right]\end{bmatrix}$$

$$\mathbf{I}_{\mathrm{DDC}}(t) = \begin{bmatrix}i_{\mathrm{DDC}}^a(t)\\ i_{\mathrm{DDC}}^b(t)\\ i_{\mathrm{DDC}}^c(t)\end{bmatrix} = \begin{bmatrix}I_0^a\\ I_0^b\\ I_0^c\end{bmatrix}e^{-\sigma t},$$

and the superscripts $+$ and $-$ represent positive and negative sequence quantities, respectively.

Analogous to (2), the three-phase sum current vector is

$$\mathbf{I}_{\mathrm{r}}(t) = \mathbf{I}(t) + \mathbf{I}(t - T/2) \tag{8}$$

Accordingly, entries of the DDC current vector can be obtained as (with $m = a, b, c$)

$$i_{\mathrm{DDC}}^m(t) = \frac{I_{\mathrm{tr}}^m(t)}{1 + \left(\frac{\int_{t-2L}^{t} I_{\mathrm{tr}}^m(t)\mathrm{d}t}{\int_{t-L}^{t} I_{\mathrm{tr}}^m(t)\mathrm{d}t} - 1\right)^{\frac{T}{2L}}} \tag{9}$$

When transformed to *dq*-frame with rotational speed ω, the positive-sequence fundamental frequency component is converted into a DC signal, while negative-sequence components and harmonics remain the form of AC waves, which can be utilized for signal separation. In compact form, the transient currents can be transformed into *dq*-frame by

$$\mathbf{I}^{dq}(t) = \mathbf{T}_{3\mathrm{s/2r}}\mathbf{I}(t) \tag{10}$$

where $\mathbf{I}^{dq}(t) = \left[i_{\mathrm{tr}}^d(t) \quad i_{\mathrm{tr}}^q(t)\right]^{\mathrm{T}}$,

$$\mathbf{T}_{3\mathrm{s/2r}} = \frac{2}{3}\begin{bmatrix}\sin\omega t & \sin\left(\omega t - 2\pi/3\right) & \sin\left(\omega t + 2\pi/3\right)\\ \cos\omega t & \cos\left(\omega t - 2\pi/3\right) & \cos\left(\omega t + 2\pi/3\right)\end{bmatrix}.$$

Accordingly, transient currents in *dq*-frame yield

$$\begin{cases} i_{\mathrm{tr}}^d(t) = I_1^+\cos\varphi_1^+ + i_{\mathrm{DDC}}^d(t) - i_{\mathrm{even}}^d(t)\\ i_{\mathrm{tr}}^q(t) = I_1^+\sin\varphi_1^+ + i_{\mathrm{DDC}}^q(t) + i_{\mathrm{even}}^q(t)\end{cases} \tag{11}$$

where i_{even}^d and i_{even}^q are given by (12) at the top of the next page (with $k = 1, 2, 3, \ldots$), and

$$\begin{cases} i_{\mathrm{DDC}}^d(t) = \frac{2}{3}\left[I_0^a\sin\omega t + I_0^b\sin\left(\omega t - 2\pi/3\right)\right.\\ \qquad\qquad \left. + I_0^c\sin\left(\omega t + 2\pi/3\right)\right]e^{-\sigma t}\\ i_{\mathrm{DDC}}^q(t) = \frac{2}{3}\left[I_0^a\cos\omega t + I_0^b\cos\left(\omega t - 2\pi/3\right)\right.\\ \qquad\qquad \left. + I_0^c\cos\left(\omega t + 2\pi/3\right)\right]e^{-\sigma t}\end{cases} \tag{13}$$

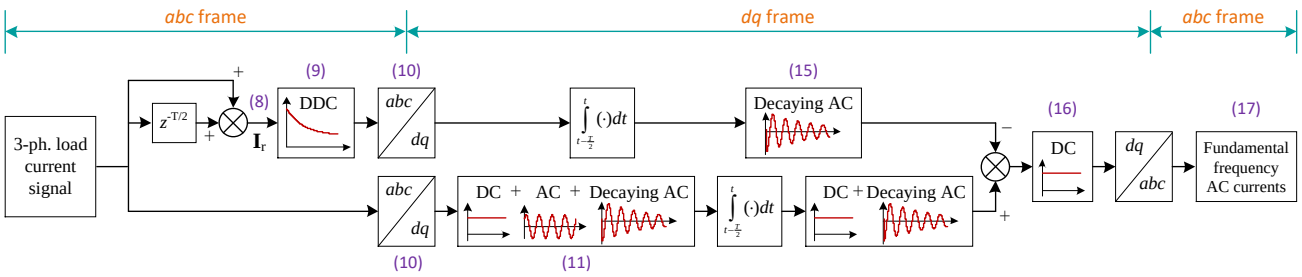

Fig. 1. Graphical representation of the proposed algorithm deduction.

$$
\begin{aligned}
i^{d}_{\text{even}}(t)&=I_1^{-}\cos\left(2\omega t+\varphi_1^{-}\right)-\sum_{n=6k+1}I_n^{+}\cos\left[(n-1)\,\omega t+\varphi_n^{+}\right]+\sum_{n=6k-1}I_n^{+}\cos\left[(n+1)\,\omega t+\varphi_n^{+}\right]+\sum_{n=6k+1}I_n^{-}\cos\left[(n+1)\,\omega t+\varphi_n^{-}\right]-\sum_{n=6k-1}I_n^{-}\cos\left[(n-1)\,\omega t+\varphi_n^{-}\right]\\
i^{q}_{\text{even}}(t)&=I_1^{-}\sin\left(2\omega t+\varphi_1^{-}\right)+\sum_{n=6k+1}I_n^{+}\sin\left[(n-1)\,\omega t+\varphi_n^{+}\right]+\sum_{n=6k-1}I_n^{+}\sin\left[(n+1)\,\omega t+\varphi_n^{+}\right]+\sum_{n=6k+1}I_n^{-}\sin\left[(n+1)\,\omega t+\varphi_n^{-}\right]+\sum_{n=6k-1}I_n^{-}\sin\left[(n-1)\,\omega t+\varphi_n^{-}\right]
\end{aligned}
\tag{12}
$$

Hence, the transient impact currents in *dq*-frame encompass i) a DC part corresponding to positive-sequence fundamental frequency AC component, ii) a decaying AC part corresponding to DDC component and iii) even harmonics corresponding to the negative-sequence fundamental frequency AC component, and corresponding to the positive-/negative-sequence odd harmonics. The even harmonics in *dq*-frame can be canceled via full-wave symmetry, i.e.

$$
\int_{t-\frac{T}{2}}^{t} i_{\text{even}}\left(\cdot\right)dt\equiv 0 \tag{14}
$$

where $i_{\text{even}}\left(\cdot\right)$ represents an even harmonic current component.

The *dq*-frame decaying AC part can be calculated by

$$
\begin{cases}
\displaystyle\int_{t-\frac{T}{2}}^{t} i^{d}_{\text{DDC}}\left(t\right)dt=\frac{1}{2}\mathbf{T}_{\text{2s/1r}}\mathbf{H}_{\sigma\omega}\mathbf{C}^{\text{d}}_{3/2}\mathbf{I}_{\text{r}}\\
\displaystyle\int_{t-\frac{T}{2}}^{t} i^{q}_{\text{DDC}}\left(t\right)dt=\frac{1}{2}\mathbf{T}_{\text{2s/1r}}\mathbf{H}_{\sigma\omega}\mathbf{C}^{\text{q}}_{3/2}\mathbf{I}_{\text{r}}
\end{cases}
\tag{15}
$$

where $\mathbf{T}_{\text{2s/1r}}=\frac{2}{3}\begin{bmatrix}\sin\left(\omega t\right) & \cos\left(\omega t\right)\end{bmatrix}$, $\mathbf{H}_{\sigma\omega}=\frac{1}{\sigma^2+\omega^2}\begin{bmatrix}\sigma & \omega\\ \omega & -\sigma\end{bmatrix}$, $\mathbf{C}^{\text{d}}_{3/2}=\begin{bmatrix}-2 & 1 & 1\\ 0 & -\sqrt{3} & \sqrt{3}\end{bmatrix}$, $\mathbf{C}^{\text{q}}_{3/2}=\begin{bmatrix}0 & -\sqrt{3} & \sqrt{3}\\ 2 & -1 & -1\end{bmatrix}$.

Accordingly, by time integral of (11) over half grid period and subtracting (15), the DC part in (11) can be obtained as

$$
\begin{cases}
I_1^{+}\cos\varphi_1^{+}=\dfrac{1}{T}\left(2\displaystyle\int_{t-\frac{T}{2}}^{t} i^{d}_{\text{tr}}\left(t\right)dt-\mathbf{T}_{\text{2s/1r}}\mathbf{H}_{\sigma\omega}\mathbf{C}^{\text{d}}_{3/2}\mathbf{I}_{\text{r}}\right)\\
I_1^{+}\sin\varphi_1^{+}=\dfrac{1}{T}\left(2\displaystyle\int_{t-\frac{T}{2}}^{t} i^{q}_{\text{tr}}\left(t\right)dt-\mathbf{T}_{\text{2s/1r}}\mathbf{H}_{\sigma\omega}\mathbf{C}^{\text{q}}_{3/2}\mathbf{I}_{\text{r}}\right)
\end{cases}
\tag{16}
$$

Therefore, the positive-sequence fundamental frequency AC currents yield

$$
\mathbf{I}_1^{+}\left(t\right)=\frac{1}{T}\mathbf{T}^{-1}_{\text{3s/2r}}\left(2\int_{t-\frac{T}{2}}^{t}\mathbf{I}^{dq}\left(t\right)dt-\begin{bmatrix}\mathbf{T}_{\text{2s/1r}}\mathbf{H}_{\sigma\omega}\mathbf{C}^{\text{d}}_{3/2}\mathbf{I}_{\text{r}}\\ \mathbf{T}_{\text{2s/1r}}\mathbf{H}_{\sigma\omega}\mathbf{C}^{\text{q}}_{3/2}\mathbf{I}_{\text{r}}\end{bmatrix}\right) \tag{17}
$$

For removal of components other than the positive-sequence fundamental-frequency current in the utility grid, the difference between the transient load current and the extracted positive-sequence fundamental frequency signal (17) is served as the APF current reference, i.e.

$$
\mathbf{I}_{\text{APF}}\left(t\right)=\mathbf{I}_1^{-}\left(t\right)+\mathbf{I}_{\text{h}}\left(t\right)+\mathbf{I}_{\text{DDC}}\left(t\right)=\mathbf{I}\left(t\right)-\mathbf{I}_1^{+}\left(t\right) \tag{18}
$$

With the proposed scheme, the overall detection time has been reduced from 1 to 0.5 grid cycle w.r.t. existing techniques. The response time is mainly spent on the cascaded AC canceling block (with $0.5T$ delay) and DDC canceling block (with $2L$ delay that can be neglected for short L).

III. Enhanced APF and Verification

To identify the DDC event, the pertinent status signal S is firstly defined. Specifically, if the DDC component is smaller than a certain level, i.e.

$$
\begin{cases}
\left|i_{\text{tr}}\left(t\right)-i_{\text{tr}}\left(t-T\right)\right|<I_{\text{th}}\\
\left|i_{\text{tr}}\left(t\right)+i_{\text{tr}}\left(t-T/2\right)\right|<I_{\text{th}}
\end{cases},
\tag{19}
$$

the status signal S is set to 1; otherwise, $S=0$. Here, I_{th} is the detection threshold, which can be designed as follows.

Considering that the amplitude of DDC component in larger in the first half cycle, where the interference to the fundamental frequency AC signal of the power grid (with RMS value $I=I_1/\sqrt{2}$) is the largest, this interval is chosen in this paper to calculate the RMS value of DDC current (denoted as I_{DDC} and corresponds to the energy of the DDC component). The effect of the DDC component is evaluated, and the threshold current is designed, both from the perspective of energy. To this end, I_{DDC} is calculated as

$$
I_{\text{DDC}}=\sqrt{\frac{2}{T}\int_0^{\frac{T}{2}} i^2_{\text{DDC}}\left(t\right)\mathrm{d}t}=I_0\sqrt{\frac{1-e^{-\sigma T}}{\sigma T}} \tag{20}
$$

Besides, let $t=T/2$ and consider (2) and (20), we have

$$
I_{\text{tr}}\left(T/2\right)=I_0\left(1+e^{-\frac{\sigma T}{2}}\right)=I_{\text{DDC}}\sqrt{\frac{\sigma T}{1-e^{-\sigma T}}}\left(1+e^{-\frac{\sigma T}{2}}\right) \tag{21}
$$

Since the signal-to-noise ratio $\eta=I/I_{\text{DDC}}$ in industrial applications is usually required to reach a standard value η_{min}, the interference of DDC component is large (and the DDC suppression function should be triggered) when I_{DDC} reaches I/η_{min}. Besides, since σT is usually small, the exponential term in (21) can be simplified by a first-order Taylor series expansion. By also considering (19) and (21), the threshold current can be obtained as

$$
I_{\text{th}}=\frac{I}{\eta_{\text{min}}}\sqrt{\frac{\sigma T}{1-e^{-\sigma T}}}\left(1+e^{-\frac{\sigma T}{2}}\right)\approx\frac{2I}{\eta_{\text{min}}} \tag{22}
$$

To absorb the DDC caused impact currents, the traditional APF functionality can be extended to the compensation of harmonics as well as DDC component in the event of transient, i.e. when $S=0$. In the steady-state condition or with a negligible DDC component, i.e. when $S=1$, the traditional APF is adopted. Thus the complete APF control strategy with the proposed detection algorithm is obtained in Fig. 2.

To verify the effectiveness of the proposed scheme, harmonics and DDC components are simultaneously considered in the experiment system whose structure, parameters and the detailed procedure used to introduce DDC currents can be found in [1]. Specifically, $I_{\text{th}}=1$ A is adopted in this paper.

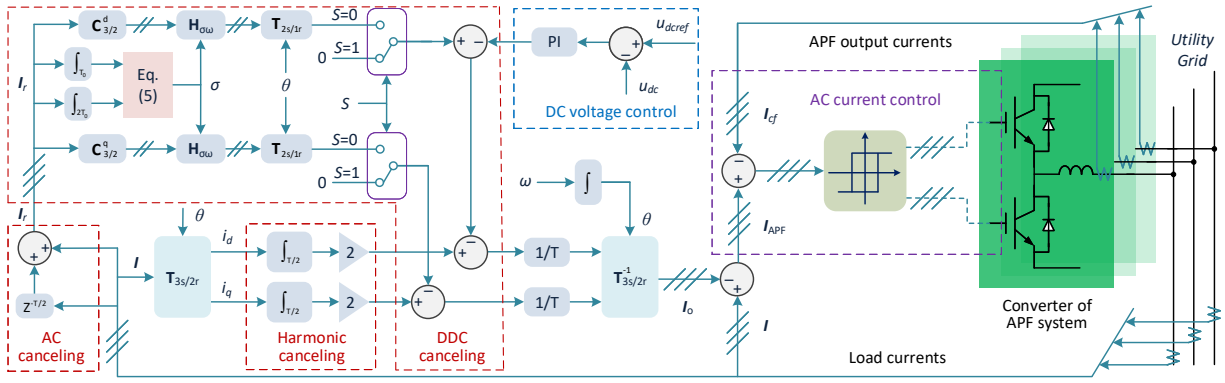

Fig. 2. Enhanced APF control diagram with proposed detection scheme.

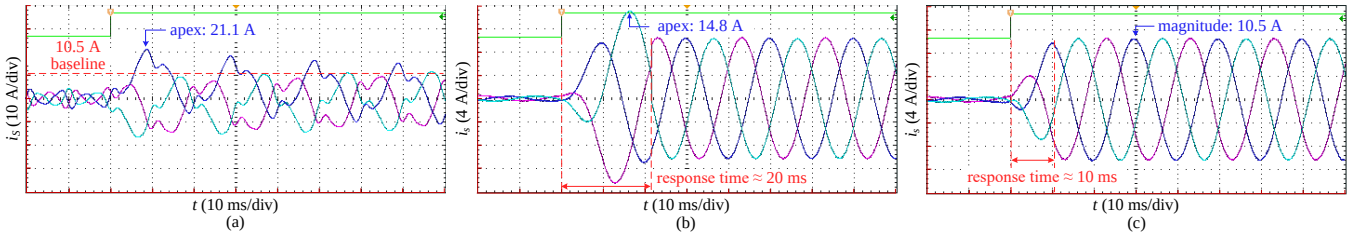

Fig. 3. Grid-side currents in experiments (a) without APF, (b) with APF and DDC detection technique in [1], and (c) with APF and the proposed scheme.

As shown in Fig. 3(a), the grid-side currents have significant harmonics and asymmetric DDC components caused by the nonlinear and impact loads, and they can introduce serious PQ issues. If the APF simultaneously compensates the DDC and harmonic currents, the distortion and asymmetry issues of the grid-side current can be solved effectively. The developed strategy, with a significantly reduced response time of about 0.5 grid cycle [see Fig. 3(c)], enables APF to effectively suppress the grid impact current and smooth the current transition. The maximum current amplitude has been reduced by half, i.e. from 21.1 A to 10.5 A [see Fig. 3(a) and (c)]. In addition, it is worth highlighting that the reduced response time is of paramount importance for avoiding the maximum grid-side surge current during 0.5 to 1 grid cycle after the introduction of DDC component, if compared to a conventional technique with detection time of 1 grid cycle [see Fig. 3(b) and (c)].

IV. Conclusion

In this paper, a novel DDC component detection algorithm is developed, providing superior performance in both response time and detection precision. With the proposed extension, existing APFs can be readily used to provide additional ability in the presence of DDC component, effectively stabilizing the utility grid by annihilating the impact grid current and by smoothing current transition. Experimental results verified the feasibility and advancement of the proposed methodology.

References

[1] L. Xiong, X. Liu, C. Zhao, and F. Zhuo, "A fast and robust real-time detection algorithm of decaying dc transient and harmonic components in three-phase systems," *IEEE Trans. Power Electron.*, vol. 35, no. 4, pp. 3332–3336, 2020.

[2] K. Zhu and P. W. T. Pong, "Fault classification of power distribution cables by detecting decaying DC components with magnetic sensing," *IEEE Trans. Instrum. Meas.*, vol. 69, no. 5, pp. 2016–2027, 2020.

[3] C. Sun, G. Joos, and F. Bouffard, "Adaptive coordination for power and SoC limiting control of energy storage in an islanded AC microgrid with impact load," *IEEE Trans. Power Deliv.*, vol. 35, no. 2, pp. 580–591, 2020.

[4] M. Pazoki, "A new DC-offset removal method for distance-relaying application using intrinsic time-scale decomposition," *IEEE Trans. Power Del.*, vol. 33, no. 2, pp. 971–980, 2018.

[5] Z. Jiang, S. Miao, and P. Liu, "A modified empirical mode decomposition filtering-based adaptive phasor estimation algorithm for removal of exponentially decaying DC offset," *IEEE Trans. Power Del.*, vol. 29, no. 3, pp. 1326–1334, 2014.

[6] B. Jafarpisheh, S. M. Madani, and S. Jafarpisheh, "Improved DFT-based phasor estimation algorithm using down-sampling," *IEEE Trans. Power Del.*, vol. 33, no. 6, pp. 3242–3245, Dec. 2018.

[7] D. Celeita, J. D. Perez, and G. Ramos, "Assessment of a decaying dc offset detector on cts measurements applying mathematical morphology," *IEEE Trans. Ind Appl*, vol. 55, no. 1, pp. 248–255, 2019.

[8] U. Subudhi, H. K. Sahoo, and S. K. Mishra, "Harmonics and decaying DC estimation using volterra LMS/F algorithm," *IEEE Trans. Ind Appl*, vol. 54, no. 2, pp. 1108–1118, Mar. 2018.

[9] C.-C. Chen and Y.-Y. Hsu, "A novel approach to the design of a shunt active filter for an unbalanced three-phase four-wire system under nonsinusoidal conditions," *IEEE Trans. Power Deliv.*, vol. 15, no. 4, pp. 1258–1264, 2000.